Optical Snakes and Ladders: Dispersion and nonlinearity in microcoil resonators

N. G. R. Broderick
Optoelectronics Research Centre, University of Southampton, Southampton SO17 1BJ, UK
ngb@orc.soton.ac.uk

Abstract: Microcoil resonators are a radical new geometry for high Q resonators with unique linear features. In this paper I briefly summarise their linear properties before extending the analysis to nonlinear interactions in microcoil resonators. As expected such nonlinear resonators are bistable and exhibit hysteresis. Finally I discuss possible applications and extensions to such resonators.

OCIS codes: (190.4370) Nonlinear optics, fibers, (060.2340) Fiber optics components

References and links

1. M. Sumetsky, "Optical fiber microcoil resonator," Optics Express **12,** 2303 (2004).
2. M. Sumetsky, "Uniform coil optical resonator and waveguide: transmission spectrum, eigenmodes, and dispersion relation," Optics Express **13,** 4331 (2005).
3. M. Sumetsky, "Basic elements for microfiber photonics: Micro/nanofibers and microfibre coil resonators," IEEE J. Light. Tech. **26,** 21–27 (2008).
4. F. Xu and G. Brambilla, "Manufacture of 3-D microfiber coil resonators," IEEE Photonics Technology Letters **19,** 1481–1483 (2007).
5. F. Xu and G. Brambilla, "Embedding optical microfiber coil resonators in Teflon," Opt. Lett. **32,** 2164–2166 (2007).
6. F. Xu, P. Horak, and G. Brambilla, "Optimised design of microcoil resonators," IEEE J. Light. Tech. **25,** 1561–1567 (2007).
7. It should be noted that there are at least two misprints in Sumetsky's Optics Express paper [2]. Firstly in Eq. 1 there is a factor i missing on the L.H.S. Secondly in the equation for the transmission a factor of $\exp(i\beta l)$ is missing. Both of these misprints do not occur in his original paper.
8. G. P. Agrawal, *Nonlinear Fibre Optics*, 3rd ed. (Academic Press, San Diego, 2001).
9. A. B. Aceves, C. DeAngelis, T. Peschel, R. Muschall, F. Lederer, S. Trillo, and S. Wabnitz, "Discrete self-trapping, soliton interactions and beam steering in nonlinear waveguide arrays," Phys. Rev. E **53,** 1172–1189 (1996).
10. K. Ogusu, "Dynamic Behavior of Reflection Optical Bistability in a Nonlinear Fiber Ring Resonator," IEEE J. Quant. Elect. **32,** 1537–1543 (1996).
11. Q. Xu and M. Lipson, "Carrier-induced optical bistability in silicon ring resonators," Opt. Lett. **31,** 341–343 (2006).
12. J. Nocedal and S. J. Wright, *Numerical Optimisation*, 1st ed. (Springer-Verlag, New York, 1999).

1. Introduction

Recently Sumetsky[1, 2] proposed and described a new type of optical resonator, the optical microcoil resonator (OMR). The OMR consists of a tapered micron diameter fibre coiled up so that light can couple from one turn to the next as shown in Fig. 1. In this resonator light can travel up in two different ways - either by propagating along the length of the fibre or, more quickly, by coupling from one coil to the next. Similarly light can descend by coupling from one coil to the coil below. It can be thought of as the optical equivalent of a game of

#99852 - $15.00 USD Received 5 Aug 2008; revised 27 Aug 2008; accepted 1 Sep 2008; published 26 Sep 2008

snakes and ladders where the coupling plays the role of the snakes and ladders while the linear propagation corresponds to taking the long route to the top. Just as a game of snakes and ladders need never end with the player alternatively ascending ladders and descending snakes so light can get trapped in a OMR by coupling up and down in equal measures. Taking the analogy to extremes the randomness produced by the dice in the game can be thought of as mimicking the behaviour of a single photon in the device which take a random trajectory through the resonator.

Since being introduced by Sumetsky, OMRs have been demonstrated experimentally by a number of authors[3, 4, 5] and have been proposed as sensors due to their high Q values and large evanescent fields. In particular compared to other high Q cavities OMR are attractive due to the ease of coupling light into and out of them (particularly simple since they are made from tapered SMF28 with fibre pigtails at each end). In this paper I extend the previous analysis to look at the nonlinear properties of OMR as well as discussing the linear properties in some detail.

2. Theoretical model

Following the analysis of Sumetsky[2] light propagating round a uniform microcoil with n turns in the linear regime is described by the following set of equations:

$$-i\frac{d}{ds}\begin{pmatrix} A_1 \\ A_2 \\ A_3 \\ \vdots \\ A_{n-1} \\ A_n \end{pmatrix} = \begin{pmatrix} 0 & \kappa & 0 & 0 & \dots & 0 & 0 \\ \kappa & 0 & \kappa & 0 & \dots & 0 & 0 \\ 0 & \kappa & 0 & \kappa & \dots & 0 & 0 \\ \vdots & \vdots & \vdots & \vdots & \dots & \vdots & \vdots \\ 0 & 0 & \dots & 0 & \kappa & 0 & \kappa \\ 0 & 0 & 0 & \dots & 0 & \kappa & 0 \end{pmatrix} \begin{pmatrix} A_1 \\ A_2 \\ A_3 \\ \vdots \\ A_{n-1} \\ A_n \end{pmatrix} \tag{1}$$

where $A_k(s)$ is the slowly varying amplitude of the electric field in the kth coil at a distance s round the coil and κ is the usual coupling constant between two adjacent waveguides. Since at the end of each loop the output of the k coil must equal the input of the $k+1$ coil this implies that

$$\begin{pmatrix} A_1(0) \\ A_2(0) \\ A_3(0) \\ \vdots \\ A_{n-1}(0) \\ A_n(0) \end{pmatrix} = \begin{pmatrix} 0 & 0 & 0 & \dots & 0 & 0 \\ e^{i\beta l} & 0 & 0 & \dots & 0 & 0 \\ 0 & e^{i\beta l} & 0 & \dots & 0 & 0 \\ \vdots & \vdots & \vdots & \dots & \vdots & \vdots \\ 0 & 0 & 0 & \dots & 0 & 0 \\ 0 & 0 & 0 & \dots & e^{i\beta l} & 0 \end{pmatrix} \begin{pmatrix} A_1(l) \\ A_2(l) \\ A_3(l) \\ \vdots \\ A_{n-1}(l) \\ A_n(l) \end{pmatrix} + \begin{pmatrix} A_1(0) \\ 0 \\ 0 \\ \vdots \\ 0 \\ 0 \end{pmatrix} \tag{2}$$

where β is the propagation constant of the mode and l is the length of each coil. The input to the coil is given by $A_1(0)$ while the output is given by $A_n(l)e^{i\beta l}$. The transmission coefficient is defined as:

$$T = A_n(l)e^{i\beta l}/A_1(0). \tag{3}$$

Note that for a lossless system $|T| = 1$ while one can describe the effects of loss through an imaginary propagation constant $\beta = 2\pi/\lambda + i\alpha$ where α represents the loss. Fig. 1 shows a typical transmission spectrum for a lossy OMR with 8 coils and with $\kappa = 5\,\mathrm{mm}^{-1}$ and $l = 1\,\mathrm{mm}$. Introducing loss into the system not only makes the model more realistic but also provides a useful guide to understanding the resonant behaviour of the OMR. In the lossy case resonances lead to light having a longer effective path length and so experiences more loss leading to a drop in transmission.

#99852 - $15.00 USD Received 5 Aug 2008; revised 27 Aug 2008; accepted 1 Sep 2008; published 26 Sep 2008

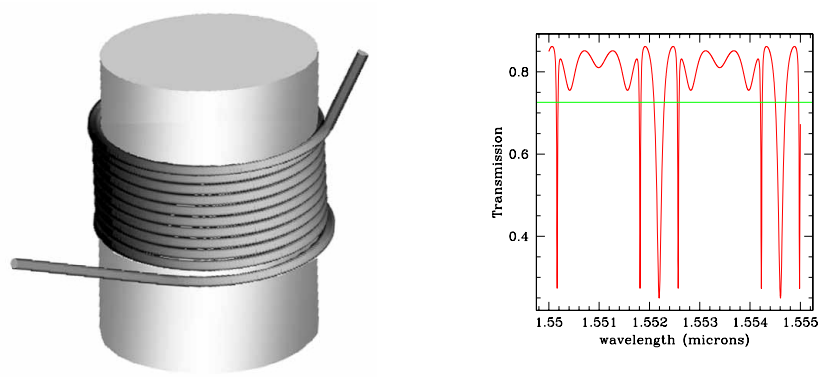

Fig. 1. (a) Schematic of a microcoil resonator taken from [2]. (b) Transmission spectrum for a lossy OMR with 8 coils. The loss is $0.02\,\mathrm{dB/mm}$ while the coupling strength was $3\,\mathrm{mm}^{-1}$. The green line shows the expected transmission for a straight length of fibre with the same length and loss.

It is possible to solve Eq. (1) and Eq. (2) as follows. Rewriting Eq. (2) in compact form gives

$$\mathbf{A}(0) = B\mathbf{A}(l) + \mathbf{A}_{in} \tag{4}$$

while the solution of Eq. (1) is given by

$$\mathbf{A}(l) = K(l)\mathbf{A}(0) \tag{5}$$

where $\mathbf{A}$ is a column vector of the amplitudes A_k and K is the formal matrix exponent of the coupling matrix in Eq. (1). Eq. (4) and Eq. (5) can be solved simultaneously giving

$$\mathbf{A}(l) = [I - K(l)B]^{-1} K(l)\mathbf{A}_{in} \tag{6}$$

$$\mathbf{A}(0) = [I - BK(l)]^{-1} \mathbf{A}_{in} \tag{7}$$

$$\mathbf{A}(s) = K(s)\,[I - BK(l)]^{-1} \mathbf{A}_{in} \tag{8}$$

Note that this solution should be formally identically to the one given by Sumetsky in [2, 7].

2.1. Group velocity and dispersion of Microcoil resonators

Although the linear properties of OMR are all implicitly in the solution given by Sumetsky [2] it is useful to draw out these properties and show explicitly some of the novel linear properties of OMRs before discussing nonlinear OMRs. As with any all-pass resonator one can define the group delay t_d as the derivate of the phase of the transmission with frequency. Writing the transmission as $T = t\exp[i\phi(\omega)]$ the group delay is then given by

$$t_d = \frac{d\phi}{d\omega} \tag{9}$$

and similarly I define an effective group velocity as the total length of the resonator l divided by the time delay.

$$v_g = l/\frac{d\phi}{d\omega} \tag{10}$$

#99852 - $15.00 USD Received 5 Aug 2008; revised 27 Aug 2008; accepted 1 Sep 2008; published 26 Sep 2008

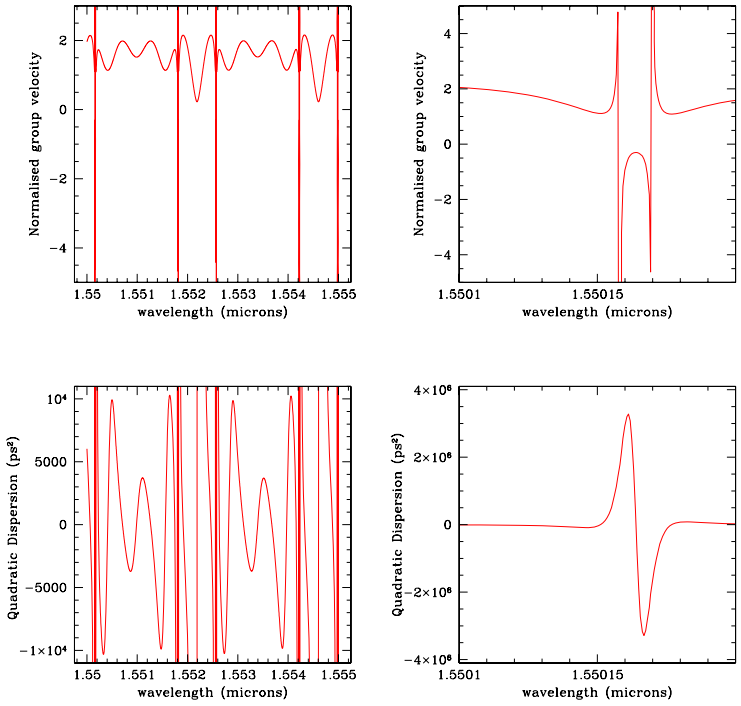

Fig. 2. Normalised group velocity (top row) and dispersion (bottom) for a 8 turn OMR with the same parameters as the one shown in Fig. 1. The figures on the right are expanded versions of the main graphs showing the narrow wavelength region of negative group velocity. Note that off resonance the dispersion is still large (1000's of picoseconds squared) and increases by several orders of magnitude on resonance. In the graphs the spikes are due to numerical errors at points where the group velocity becomes undefined.

while the dispersion of the resonator is then given by the derivate of the effective group velocity. The normalised group velocity and dispersion of a typical microcoil resonator are shown in Fig. 2 where a normalised velocity of unity corresponds to the speed of light in the isolated fibre (i.e. c/n_{eff}). The first thing to notice about the group velocity is that typically it is greater than unity. This shows that for most wavelengths light takes a short cut through the resonator by coupling from one coil to the next (i.e. the same as going up a ladder) and so the length it "sees" is less than the physical resonator length. This can also be seen in the transmission spectrum where off resonance the transmission is greater than $\exp(-2\alpha l)$ which is the expected loss of the OMR. In the lossy case one can define an effective length by

$$t(\omega)^2 = |e^{-\alpha l_{eff}(\omega)}|^2 \tag{11}$$

where t^2 is the absolute value squared of the transmission.

More interestingly there are distinct regions where the group velocity can be significantly less than unity and also regions where the group velocity is negative. The regions of slow light can be understand as corresponding to resonances of the microcoil, that is slow light occurs near the values of β and κ for which

$$det(I - BK) = 0. \tag{12}$$

#99852 - $15.00 USD Received 5 Aug 2008; revised 27 Aug 2008; accepted 1 Sep 2008; published 26 Sep 2008

At these points resonator modes exist (defined by $A_1(0) = A_n(l) = 0$ and $|\mathbf{A}| > 0$) which store energy indefinitely in the OMR. The regions of negative group velocity are harder to interpret physically but correspond to regions where the transmitted phase decreases with frequency.

Looking at the dispersion of the OMR in Fig. 2 it can be seen that it is extremely high across the entire spectrum. The reason for this is that when the light is off-resonance it typically couples from one coil to the next and so the effective length is a strong function of frequency leading to a large dispersion. Then close to resonance where the group velocity drops to zero the dispersion becomes much larger due to resonance effects but only over a very narrow wavelength range and indeed at these wavelengths the loss increases as well. It is expected that by using non-uniform microcoil resonators similar to those discussed in [6] the dispersion characteristics of the resonators could be tailored to meet specific requirements whether for phase-matching or for dispersion compensation. However here I am interested in their nonlinear properties.

3. Nonlinear Microcoil resonators

In the previous section I described briefly the linear properties of optical microcoil resonators. Of particular interest are the regions where the group velocity decreases due to resonance effects. At these frequencies a large amount of light is stored in the OMR leading to high internal optical intensities. Clearly in these cases as in other optical resonators nonlinear effects will be enhanced and so it is important to understand their effects. In addition nonlinear effects are enhanced compared to standard fibres due to the small fibre diameter and hence small effective area. Here I consider only the simplest case of a Kerr nonlinearity and CW light although clearly more complicated nonlinearity interactions could also be considered.

Following the standard derivation of the nonlinear coupled mode equations for n nonlinear waveguide arrays with a Kerr nonlinearity[8, 9] gives the expected set of coupled equations:

$$\frac{dA_1}{ds} = -\alpha A_1 + i\gamma|A_1(s)|^2 A_1(s) + i\kappa A_2(s) \tag{13a}$$

$$\frac{dA_k}{ds} = -\alpha A_k + i\gamma|A_k(s)|^2 A_j(s) + i\kappa[A_{k-1}(s) + A_{k+1}(s)] \tag{13b}$$

$$\frac{dA_n}{ds} = -\alpha A_n + i\gamma|A_n(s)|^2 A_n(s) + i\kappa A_{n-1}(s) \tag{13c}$$

where γ is the usual nonlinear coefficient and is proportional to the appropriate element of the χ^3 suseptability tensor and $A_k(s)$ represents the slowly varying amplitude of the light in the kth coil as before. Here I have explicitly included the loss α in the equations. Again the boundary conditions given by Eq. (2) hold. Note that renormalising the field amplitudes by $A_k \to 1/\sqrt{\gamma}A_k$ sets the effective nonlinear coefficient to unity which is done in the numerical simulations. Writing the formal solution to Eq. (13) as $\mathbf{A}(l) = N(\mathbf{A})\mathbf{A}(0)$ the only possible self consistent solutions obey

$$\mathbf{A}(0) = BN(\mathbf{A})\mathbf{A}(0) + \mathbf{A}_{in} \tag{14}$$

where B is given by Eq. (2). The numerical approach used to find these solutions is discussed in Appendix 1.

It should be noted that the case of a single loop coil was studied by Ogusu[10] who found that in the nonlinear regime the coil exhibited bistability and hysteresis. Similarly it is well known that lossy ring resonators also exhibit bistable behaviour in the nonlinear regime (for example see [11]). Hence it is to be expected that the NOMR will also exhibit bistable behaviour and hysteresis. This is indeed what is found as shown in Fig. 3 which shows the bistable behaviour for a microcoil resonator with 3 turns for a variety of wavelengths. Here the loss was $0.02\,\mathrm{dB/mm}$ and the diameter of the coils was $1\,\mathrm{mm}$ while the coupling coefficient was

#99852 - $15.00 USD Received 5 Aug 2008; revised 27 Aug 2008; accepted 1 Sep 2008; published 26 Sep 2008

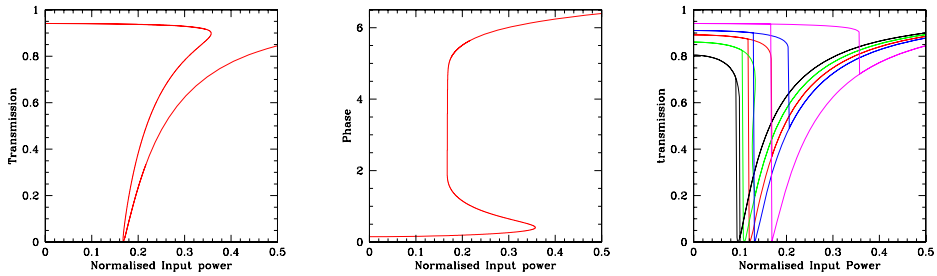

Fig. 3. Nonlinear response of a 3 turn microcoil resonator. Fig. (a) shows the full solution (both stable and unstable branches) as a function of the input power. Fig. (b) shows the output phase while Fig. (c) shows the hysteresis curves for the resonator for a range of wavelengths.

chosen so that in the linear regime the transmission is identically zero at $\lambda = 1.530\,\mu$m. While having zero transmission is not necessary it does maximise the contrast between the high and low transmission states.

Figyre 3(a) shows the transmission as a function of the normalised input power for a wavelength of $\lambda = 1.53022\,\mu$m. This is on the long wavelength size of the resonance and so one would expect the transmission to decrease as the intensity increases as can be seen. It is also clear that there is a wide range of intensities over which the transmission is no longer single valued and thus one expects the system to exhibit bistability and hysteresis. In this case the maximum contrast between the high and low transmission branches is $> 33\,$dB. The limiting factor in the contrast ratio is the fact that as the loss increases the signal intensity drops to the point where the transmission is linear thus reducing the loss. Figure 3(b) shows the output phase as a function of the input intensity and is discussed further in the appendix.

From the plots of the transmission against input power I drew hysteresis curves by noting where the transmission is single or multi-valued and assuming that physically the device will jump to a higher or lower state at that point. In all cases I assumed that the middle branch is unstable and so can be ignored (numerically the direct solutions do not converge to the middle branch indicating that while it is a fixed point it is an unstable one). This gives us the hysteresis curves plotted in Fig. 3(c) for a range of increasing wavelengths away from the resonance point. The black line shows the transmission for the closest wavelength and has the smallest hysteresis loop while the magneta line [identical to Fig. 3(a)] is the furthest away from the resonance and so has the largest region of bistability.

In Fig. 3 the amplitude was normalised so that the nonlinear coefficient is unity. In a realistic device the fibre diameter would be between $0.5\,\mu$m and $2.0\,\mu$m which implies that for a tapered SMF fibre $\gamma \approx 0.03\,\mathrm{W}^{-1}$ and so the maximum power required to see the hysteresis behaviour in Fig. 3(c) would be 16 W which is easily achievable with a pulsed microsecond source. This power could be reduced considerable by using highly nonlinear fibres or by optimising the micro-coil design (which is the subject of ongoing work).

4. Discussion and conclusions

Microcoil resonators form a fascinating geometry in which to perform optical experiments. Compared to other resonators, OMCRs posses the unique feature that although they are essentially two dimensional resonators they can only be embedded in a 3 dimensional space. In addition their linear dispersive features such as negative group velocity, slow and fast light,

#99852 - $15.00 USD Received 5 Aug 2008; revised 27 Aug 2008; accepted 1 Sep 2008; published 26 Sep 2008

high dispersion means that a wealth of nonlinear effects can easily be studied. Importantly for practical applications OMCRs are formed from tapered SMF fibres and so coupling light into and out of the resonators is a trivial task (unlike most other high Q resonators).

In this paper I have shown that OMCRs are bistable devices where the transmission depends both on the input intensity and the history of the device. Such devices can have a contrast ratio of greater than 30 dB and thus could be used in future all-optical networks. In addition the large time delays available make them attractive for all-optical delay lines where the time delay is dependent on the input intensity. In contrast to the bistability which relies on the interplay between the loss and the nonlinearity, the optical time delay does not depend on the loss and thus reductions in the loss would make such devices increasingly attractive.

Although in this paper I have only shown the results for a 3 turn nonlinear microcoil resonator, I have performed numerical simulations for OMCR with different numbers of turns and in all cases they behave in a similar fashion showing bistability and hysteresis. Concentrating on a 3 turn resonator however ensures that this behavior can be observed since 3 and 4 turn resonators can be made experimentally. It is also worth comparing the behaviour of OMCRs with more conventional ring resonators. Both devices dramatically reduce the external threshold for nonlinear effects by storing energy and thus in some ways behave similarly. However the major difference between the two is the presence of resonator modes for the micro-coil resonator in which light is stored indefinitely (in the loss-less case) leading to a theoretically infinite Q. Thus as the fabrication techniques improve and reduces the losses of micro-coil resonators the Q factors should dramatically increase making them superior to ring resonators for observing nonlinear effects.

In the future work will be done on looking at more complicated nonlinear interactions in OMCRs as well as optimising the design for optical switching. One possibility is to break the fibre in various places along the coil which would allow light to still propagate due to coupling from one coil to the next for most wavelengths but for particular wavelengths the transmission would drop dramatically. Alternatively by changing the strength of the coupling along the resonator it should be possible to apodise the device make the transmission features broader and improving the bandwidth of operation. Importantly a time-dependent set of equations should be derived since it is expected that the CW solutions will become unstable at high powers and this cannot be treated using the approach developed here.

5. Appendix 1: Numerical solutions of the nonlinear coupled mode equations

In this appendix I briefly describe the numerical approach used to solve the nonlinear coupled mode equations Eq. (14). While it is trivial to solve Eq. (13) using any standard numerical method such as the Runge-Kutta method, the problem lies in finding the appropriate starting vector to ensure that the consistency solutions are met. One approach lies in realising that Eq. (14) describes a mapping $f : \mathbb{C}^n \to \mathbb{C}^n$ given by

$$f(\mathbf{X}) = BN(\mathbf{X})\mathbf{X} + \mathbf{A}_{in}. \tag{15}$$

Noting that the desired solution is a fixed point of this mapping then under most circumstances it can be found by iterating the solution i.e.:

$$\mathbf{A}^n = BN(\mathbf{A})\mathbf{A}^{n-1} + \mathbf{A}_{in} \tag{16}$$

where $|\mathbf{A}^n - \mathbf{A}^{n-1}| \to 0$ as $n \to \infty$.

In the linear case where $N = K$ and when $\mathbf{A}^0 = \mathbf{A}_{in}$ this method results in

$$\mathbf{A}^n = \left(\sum_{k=0}^{k=n} (BK)^k \right) \mathbf{A}_{in}. \tag{17}$$

#99852 - $15.00 USD Received 5 Aug 2008; revised 27 Aug 2008; accepted 1 Sep 2008; published 26 Sep 2008

which is the formal Taylor series expansion of Eq. (7) and so this procedure will converge whenever $||BK|| < 1$. This solution technique is attractive since when $\mathbf{A}^0 = \mathbf{A}_{in}$ it mimics the physics of the situation since each iteration corresponds to another round trip of the light round the coil and so the stability of this procedure should be similar to that of the physical system. Numerical I have found this procedure to be robust but slow. However it fails completely in a number of cases such as when there is gain in the system or the solution is unstable. In these cases other methods need to be used.

In the general case a solution $\mathbf{X}$ satisfies $\mathbf{X} - f(\mathbf{X}) = 0$ which can of course be rewritten as $2n$ real equations (the real and imaginary parts of each component of the vector) and which are easily reduced to $2n-2$ real equations since the input power is given. Furthermore there are $2n-2$ unknowns being the real and imaginary parts of $A_k(0)$. This then forms a set of $2n-2$ nonlinear equations in $2n-2$ unknowns and so any standard numerical method can be used to solve them. In order to obtain the solutions presented here I have used a modified Newton's method[12] which rapidly converges to the solution given the appropriate starting point. In the cases presented here I tracked the solution while varying the input power and so fitted a parabola to the three previous solutions and then extrapolated it to provide a suitable starting point. The three initial points were found using the much slower iteration method described above. For the examples given in this paper the error given by $|\mathbf{X} - f(\mathbf{X})|^2$ is less than 10^{-15} for all points which is usually achieved by between 1 and 20 iterations of Newton's method.

A drawback of these methods is that they do not converge to unstable solutions and also that when the resonator is bistable which solution you obtain depends on the starting point. One solution to this problem can be seen using Fig. 3(b) which shows the output phase as a function of the input intensity. Importantly note that while for a given input intensity the output phase can take several values, for a given output phase there is only one unique input power which produces that phase. Thus fixing the output phase and propagating light backwards through the coil to find the input produces a unique solution allowing the full dynamics to be seen. Numerically this involves rewriting $\mathbf{X} - f(\mathbf{X}) = 0$ as $2n-1$ real equations (the additional equation is for the transmission amplitude since only the phase is known) and solving it using the same Newton's method as described previously.

Acknowledgments

The author gratefully acknowledges Dr. Peter Horak, Dr. Gilberto Brambillia and Dr. Giampaolo D'Alessandro for many helpful conversations.

#99852 - $15.00 USD Received 5 Aug 2008; revised 27 Aug 2008; accepted 1 Sep 2008; published 26 Sep 2008